Journal of NeuroVirology, 11: 144–156, 2005

ISSN: 1355-0284 print / 1538-2443 online
DOI: 10.1080/13550280590922757

Taylor & Francis
Taylor & Francis Group

Cerebrospinal fluid from human immunodeficiency virus–infected individuals facilitates neurotoxicity by suppressing intracellular calcium recovery

Rick B Meeker,[1,2] Jeramiah C Boles,[1] Kevin R Robertson,[1] and Colin D Hall[1]

[1]*Department of Neurology and* [2]*Curriculum in Neurobiology, University of North Carolina, Chapel Hill, North Carolina, USA*

Neurologic decline associated with penetration of human immunodeficiency virus type 1 (HIV-1) into the central nervous system is thought to be due, in large part, to inflammation and local secretion of neurotoxic substances. To examine the cellular processes that mediate neurotoxicity *in vivo*, the authors evaluated the ability of neurons to maintain intracellular calcium homeostasis in the presence of toxic cerebrospinal fluid (CSF) (CSF_{tox}) collected from a subset of HIV-infected individuals. Exposure of rat neural cultures to CSF_{tox} resulted in a gradual increase in intracellular calcium in neurons (+63%), microglia (+251%), and astrocytes (+52%). Pretreatment of neural cultures with CSF_{tox} resulted in an exaggerated calcium response to a brief pulse of glutamate and a >90% suppression of the rate of recovery of intracellular calcium. Attempts to model the deficit using inhibitors of calcium transport across endoplasmic reticulum, mitochondrial, or plasma membrane indicated that blockade of the plasma membrane sodium/calcium exchanger was best able to reproduce the deficits seen during exposure to CSF_{tox}. Because the inability of cells to maintain calcium homeostasis would lead to exaggerated responses from a wide variety of stimuli, therapeutics designed to facilitate calcium transport from the cell may provide more comprehensive and effective intervention than strategies targeted to specific receptor pathways. *Journal of NeuroVirology* (2005) **11,** 144–156.

Keywords: AIDS; calcium transporter; dementia; microglia; neurons; sodium/calcium exchanger

Introduction

The neurological dysfunction that develops in some individuals infected with the human immunodeficiency virus type 1 (HIV-1) is thought to be due, in large part, to the release of toxic substances from activated macrophages and microglia (Giulian *et al*, 1990; Kaul *et al*, 2001; Lipton, 1992, Pulliam *et al*, 1994; Xiong *et al* 2000). *In vitro* studies of macrophages or neural tissue infected with HIV and postmortem analyses of brain tissue have identified a number of proinflammatory substances that are elevated in response to HIV. These substances include cytokines such as tumor necrosis factor alpha (TNFα) (Graziosi *et al*, 1996; Grimaldi *et al*, 1991; Perrella *et al*, 1992; Wesselingh *et al*, 1997; Yeung *et al*, 1995), the chemokines, stromal cell-derived factor (SDF)-1α (Hesselgesser *et al*, 1998; Zheng *et al*, 1999b) and macrophage chemoattractant protein (MCP)-1 (Kelder *et al*, 1998), excitotoxins (Heyes *et al*, 1991), arachidonic acid metabolites (Genis *et al*, 1992), platelet-activating factor (Gelbard *et al*, 1994), and novel toxins (Giulian *et al*, 1996). Numerous studies have suggested that HIV proteins such as gp120 (Brenneman *et al*, 1988; Lipton *et al*, 1991; Nath and

Address correspondence to Rick Meeker, Department of Neurology, CB# 7025, 6109F Neuroscience Research Building, University of North Carolina, Chapel Hill, NC 27599, USA. E-mail: meekerr@neurology.unc.edu

This work was supported by NIH grats MH62690, AI47749, and the UNC center for AIDS Research (P30-HD37260).

Received 17 March 2004; revised 25 August 2004; accepted 1 November 2004.

Geiger 1998), gp41 (Adamson *et al*, 1999), and tat (Conant *et al*, 1998; Haughey *et al*, 1999; Magnuson *et al*, 1995; Nath and Geiger, 1998; New *et al*, 1997) may trigger the inflammatory interactions and contribute to neuronal damage. In addition, tat may directly interact with neurons to facilitate damage (Cheng *et al*, 1998). Although the above substances have been shown to promote neurotoxicity, the underlying mechanisms are still poorly understood. *In vitro* research into the mechanisms of toxicity has repeatedly implicated glutamate receptors and intracellular calcium accumulation as important factors in the etiology of neuronal damage. These conclusions are largely based on observations showing a facilitation of glutamate receptor activity or the ability of glutamate receptor antagonists to suppress the toxic activity of the compound under study. However, *most* studies suggest that the effects on glutamate receptor function are due to indirect actions of the toxin (s), although the specific pathways have not yet been identified. Perhaps the most extensive characterization of toxic activity has been done for the HIV-1 proteins gp120 and tat. In these studies, a wide range of antagonists acting on many diverse receptor and signaling pathways were found to be protective (Haughey *et al*, 1999; Holden *et al*, 1999; Zheng *et al*, 1999a).

Similar results were observed in studies designed to characterize the actions of macrophage-derived toxins. Toxins generated *in vitro* using enriched cultures of choroid plexus macrophages inoculated with the feline immunodeficiency virus (FIV) were found to induce a gradual increase in intracellular calcium followed by death of a subset of neurons (Bragg *et al*, 2002a). Pharmacological characterization of the macrophage toxins indicated that many different sources of calcium could contribute to the gradual destabilization of intracellular calcium (Bragg *et al*, 2002b). The broad profile of protective antagonists resembled results seen with gp120 (Holden *et al*, 1999) and tat (Haughey *et al*, 1999). Analysis of the kinetics of intracellular calcium changes after exposure to the toxins suggested that the destabilization of calcium was largely due to deficits in the ability to recover normal calcium homeostasis (Bragg *et al*, 2002b). Such alterations in intracellular calcium homeostasis could explain the facilitation of glutamate receptor activity as well as the diverse profile of pharmacological antagonists. If similar processes are active *in vivo*, then it makes sense that therapeutic strategies need to be targeted to downstream processes that regulate calcium homeostasis.

Like the macrophage toxins, cerebrospinal fluid (CSF) from HIV-1–infected humans (Meeker *et al*, 1999) and FIV-infected cats (Bragg *et al*, 2002a) has neurotoxic activity. To evaluate if toxic HIV+ CSF (CSF_{tox}) also induced a similar deficit in the ability of cells to recover intracellular calcium homeostasis, we applied HIV+ CSF to cultures of rat cortical neurons and measured the effects on intracellular calcium. A dramatic suppression of the ability of neurons to recover from an increase in intracellular calcium was observed that was mimicked by blockade of the plasma membrane Na^+/Ca^{2+} exchanger.

Results

Neuronal response to CSF_{tox}

On the average, most neurons responded to the CSF_{tox} with a progressive rise in intracellular calcium (late calcium destabilization), starting after about 15 to 20 min. This type of response is illustrated in Figure 1 for several neurons continuously exposed to CSF_{tox} over a period of 66 min. The image illustrates a field containing a scattered group of large and small neurons (N) as well as microglia (MG) and astrocytes (A). After exposure to CSF_{tox}, small increases in intracellular calcium were seen in several neurons (e.g., N1, N2), with peak responses between 0.1 to 0.5 min. Other neurons showed low or negligible responses (N3, N4). Although continuously exposed to the CSF_{tox}, calcium recovered to near baseline levels by 1.2 min. The first signs of the late rise in calcium were seen at 16 min. By 66 min, increases in intracellular calcium were seen in most neurons, although the magnitude of the response varied considerably (e.g., N2 versus N4) and was unrelated to the acute response (e.g., N1 versus N3). An estimate of the number of neurons with a significant delayed response to CSF_{tox} was obtained by setting a confidence limit based on the distribution of responses in control cultures treated with artificial CSF (aCSF). An individual neuronal response that was 2.57 standard deviation units above the control mean (an increase of $\geq$70.7%; 99% confidence limit) was considered to be a significant rise in intracellular calcium. Empirically, this excluded >95% of control neurons. Using this criterion, 69.8% of the neurons exposed to CSF_{tox} showed a significant rise in calcium versus 4.8% in control cultures treated with aCSF. Most of the responding cells (68.4%) showed small or negligible acute increases in calcium. The largest increases in calcium were generally accompanied by observable swelling of the neuron but only a few cells (0.9%) were observed to burst. Approximately one in five neurons (22.3%) failed to show significant changes in intracellular calcium. CSF collected from HIV-negative individuals (not illustrated) showed some activity with 25.6% of the neurons achieving the cutoff.

Calcium responses in astrocytes and microglia

The late destabilization of intracellular calcium was not restricted to neurons. Varied responses were seen in astrocytes (A) and microglia (MG), some of which are illustrated in Figure 1. One astrocyte (A) and three microglial cells (MG1 to MG3) are highlighted. In the microglia, the calcium signal was generally very low during the acute phase of the experiment (0 to 3 min), with small relative increases occasionally seen. After approximately 16 min, increases in

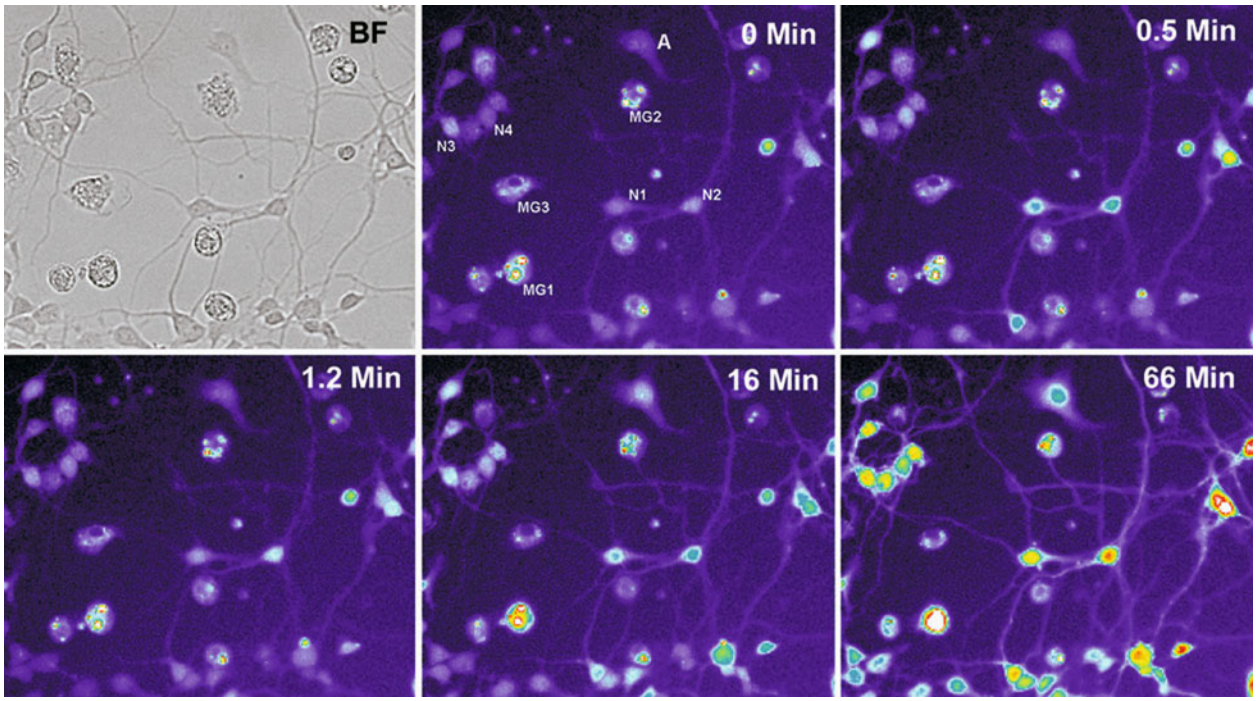

Figure 1 Increases in intracellular calcium (Fluo-3 fluorescence) in cultured rat cortical neurons (N), microglia (MG), and astrocytes (A) exposed to toxic HIV+ human CSF (CSF_{tox}). The field illustrates typical responses seen in each cell type. The brightfield image (BF) shows the morphology and location of the various cells. Basal calcium levels (fluorescence) are low prior to stimulation (0 Min). Some neurons showed modest acute increases in intracellular calcium (N1, N2), which largely recovered within 1.2 min. Other neurons (e.g., N3, N4) showed small or negligible acute increases. After 16 min, a delayed rise in intracellular calcium began with neurons achieving moderate-large increase in calcium by 66 min. The delayed increases in intracellular calcium were independent of the acute response (e.g., N1 versus N3). One astrocyte (A) and three microglial cells (MG1–3) are shown that represent the various types of responses seen following exposure to CSF_{tox}. These cells typically showed negligible acute responses to CSF_{tox}. After approximately 16 min, increases in intracellular calcium began to emerge. By 66 min, the microglia showed responses that span the range from very intense (MG1), to moderate (MG2) to negligible (MG3). An astrocyte (A) showed a small progressive rise in calcium typical of most astrocytes. Cells are pseudocolor coded for relative fluorescence intensity: white > red > yellow > green > blue > purple > black.

intracellular calcium began to emerge. After 66 min, microglia showed calcium responses ranging from intense (MG1) to mo derate (MG2) to negligible (MG3). On the average, 32.1% of the microglia responded to CSF_{tox}, with a late rise in calcium versus 5.3% in control cultures. An astrocyte (A) in the same field showed a small delayed increase in calcium in the absence of an acute response. This type of response was seen in 34.0% of the astrocytes versus 9.0% in control cultures. A few astrocytes (6.2%) showed an abrupt rapid decline in intracellular calcium and, in one case, observable blebbing (not shown). This latter observation suggested that the CSF_{tox}, may be toxic to a small subset of astrocytes. Thus, both microglia and astrocytes responded to CSF_{tox} although these responses could be quite variable from cell to cell.

A comparison of the average calcium responses of neurons, astrocytes, and microglia during continous expsure to CSF_{tox} is provided in Figure 2. Neurons showed a very small average acute increase in intracellular calcium followed by a gradual increase in the chronic phase of stimulation reaching a mean peak value 63% above baseline ($t = 3.54$, $df = 38$, $P < .001$). Microglia showed a small acute increase (15%) in intracellular calcium ($t = 2.35$, $df = 30$, $P < .05$) followed by a very large delayed increase (251%; $t = 3.34$, $df = 30$, $P < .01$). Individual microglial responses were almost always much larger than the neuronal response, although considerable cell-to-cell variability was seen (e.g., Figure 1). Although astrocytes had a much weaker signal than the neurons and microglia, the relative calcium increase was similar to that seen in the neurons (due to the very low baseline). A 52% increase ($t = 19.35$, $df = 96$, $P < .001$) was seen over time in the absence of an acute increase. However, the absolute increase in fluorescence brightness in the astrocytes was only 22% of the absolute increase in neurons and 14% of the absolute increase in microglia. The average acute response in control cultures (open symbols) was a gradual decrease in fluorescence for each cell type. During the chronic phase of stimulation, a small (13% ± 3%) but significant ($t = 4.382$, $df = 65$, $P < .001$) maximal increase in intracellular calcium was seen in the neurons (open circles), albeit at a level 4.8-fold lower than neurons stimulated with CSF_{tox}. No significant

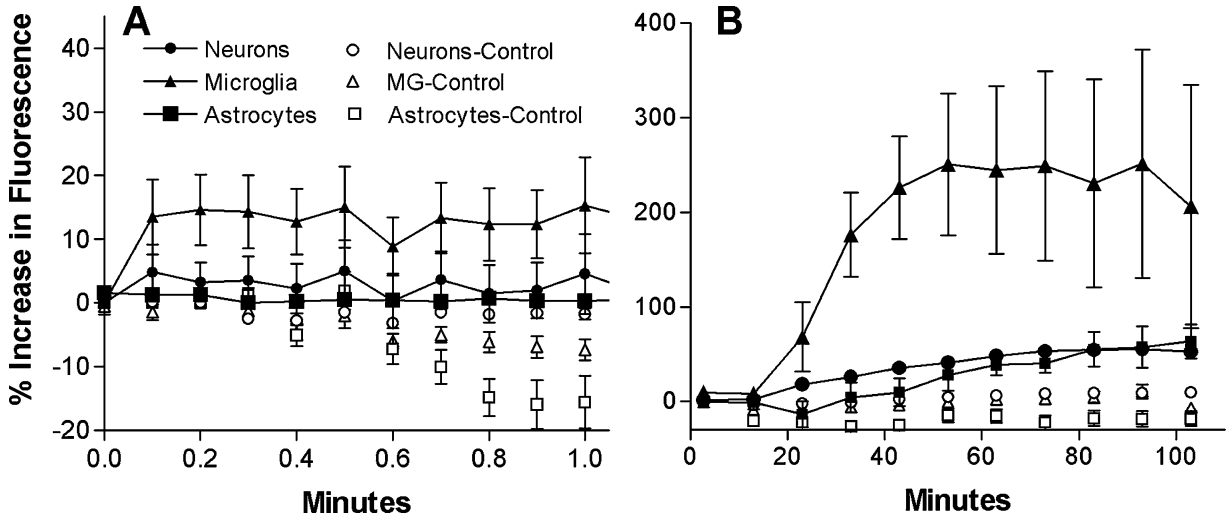

Figure 2 Summary of the average changes in intracellular calcium (% increase in Fluo-3 fluorescence) in neurons, astrocytes, and microglia following exposure to CSF_{tox}. **A**, Acute changes were minimal with only the microglia showing a significant, albeit small, increase above basal calcium. **B**, After approximately 20 min, a progressive rise in intracellular calcium was seen in all cells exposed to CSF_{tox} (note the 10-fold change in scale). The average microglial response (maximum increase = 251%, $n = 31$) greatly exceeded that of neurons (63%, $n = 39$) or astrocytes (52%, $n = 97$). The large microglial response was principally due to the high relative intensity of approximately one third of the microglia. Control cells exposed to artificial human CSF (*open symbols*) showed relatively small changes in intracellular calcium over the same time course (maximum increases: neurons, 13%, $n = 66$; astrocytes, −9%, $n = 22$; and microglia, 10%, $n = 19$).

increases were seen in the astrocytes or microglia under these conditions (open triangles and squares).

CSF_{tox} and intracellular calcium recovery

Previous studies have suggested that a prominent action of macrophage-derived toxins is the ability to inhibit the recovery of intracellular calcium (Bragg *et al*, 2002b). To assess the ability of CSF_{tox} to interfere with intracellular calcium recovery following a challenge, neural cultures were treated with CSF_{tox} for 10 min followed by the application of a brief, 6-s, pulse of 100 μM glutamate (Figure 3). To achieve a maximal effect from the brief CSF application, a 1:10 final dilution was used (Meeker *et al*, 1999). As illustrated in Figure 3A, intracellular calcium began to increase gradually during the 10-min exposure to CSF_{tox}. The glutamate pulse applied at the end of the 10-min incubation in CSF_{tox} produced a rapid increase in intracellular calcium that was 2.7-fold larger than the glutamate-induced increase seen in control cultures treated with aCSF. In the control neurons, intracellular calcium recovered to basal calcium levels within 2 min. In contrast, neurons treated with CSF_{tox} showed a slower decline that failed to return to prestimulation baseline within 6 min. The recovery profile of individual neurons exposed to CSF_{tox} was also more complex. Of a total of 158 neurons, a subset of 25 (16%) showed a prominent secondary peak after washout of the glutamate. The magnitude of this effect was large enough to be seen in the average curve. Fourteen neurons (9%) burst following the glutamate challenge while another group of 42 neurons (26%) showed a continuous increase in calcium rather than recovery. Only a few neurons (3.8%) showed rapid recovery of calcium as seen in the control condition. The remaining neurons (45.2%) showed varying intermediate rates of recovery. In spite of the individual response variation, the net effect of the CSF_{tox}, when normalized and expressed as rate of decline from peak calcium (except those that burst), was a relatively consistent decrease in the rate of recovery. Average recovery rates for the treated and control neurons are illustrated in Figure 3B. After approximately 24 s, the rate of decline in intracellular calcium stabilized at -0.0225 ± 0.0054 min^{-1} in the neurons treated with CSF_{tox} versus a decline of -0.4496 ± 0.0106 min^{-1} for the controls. This represents a 20-fold decrease in the rate of intracellular calcium recovery after exposure to the CSF_{tox}. However, because the net steady-state rate of recovery of intracellular calcium is dependent on a balance between a number of uptake and export processes, the experiments could not totally rule out the possibility that the decrease in the rate of intracellular calcium recovery might be due to an inward calcium influx that overwhelmed the clearance processes. The use of 1 μM tetrodotoxin (TTX) in these experiments minimized the likelihood that calcium influx was stimulated through synaptic influences. An estimate of the rate of calcium entry into the cell was obtained based on the ability of Mn^{2+} ions to quench FURA-2 fluorescence. Comparison of relative quench rates (rates of divalent cation influx) in neurons treated with CSF_{tox} versus control neurons (Figure 3C) indicated that influx was decreased after exposure to CSF_{tox} rather than increased. Thus, loss of calcium

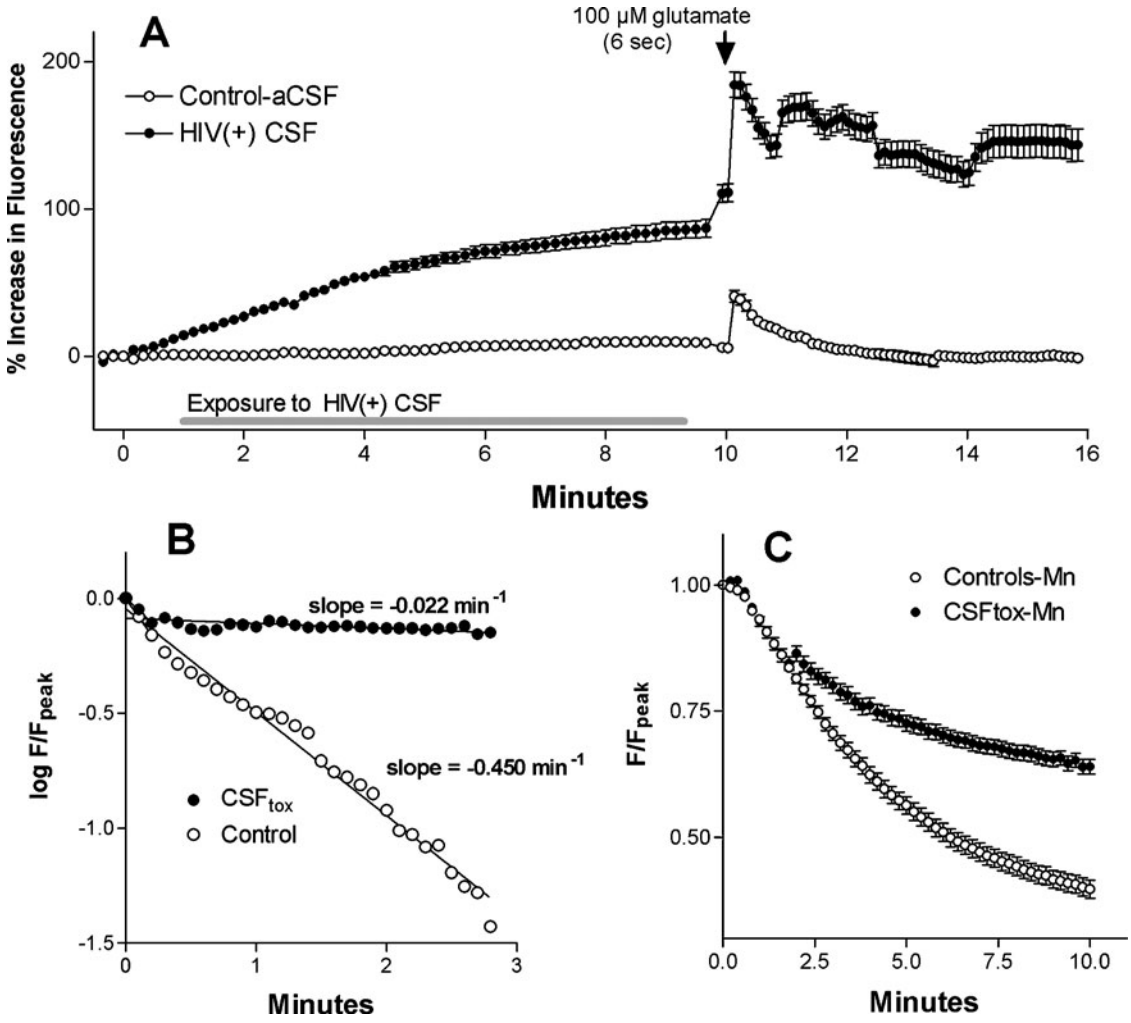

Figure 3 Intracellular calcium recovery in cultured cortical rat neurons following exposure to a brief (6-s) pulse of 100 μM glutamate applied 10 min after addition of CSF_{tox}. The CSF_{tox} was applied at a dilution of 1:10. **A**, Neurons exposed to CSF_{tox} ($n = 158$) showed a gradual accumulation of intracellular calcium and a greater and more sustained response to glutamate relative to control neurons treated with aCSF ($n = 44$). **B**, An estimate of the recovery of intracellular calcium was obtained by stimulating with a 6-s pulse of 100 μM glutamate followed by rapid washout. Fluorescence readings after glutamate washout (F) were normalized to the peak fluorescence (F_{peak}) and a log transform applied ($\log F/F_{peak}$). The resulting lines were near-linear giving rise to slope (recovery rate) estimates of -0.4496 ± 0.0106 min^{-1} for control neurons treated with aCSF ($n = 52$) and -0.0225 ± 0.0054 min^{-1} for neurons exposed to CSF_{tox} ($n = 128$). There was no overlap between the 95% confidence limits of each regression line. **C**, The rate of calcium influx was measured using Mn^{2+} quenching of FURA-2. An estimate of the initial (2 min) influx rate of -0.0590 ± 0.0005 min^{-1} for control neurons was similar to the rate of -0.0331 ± 0.0022 min^{-1} for neurons exposed to CSF_{tox}. The more extended rate component (2 to 10 min) for CSF_{tox} (-0.0094 ± 0.0005 min^{-1}, $n = 101$) was substantially lower than the estimate for control neurons ($-0.0238 + 0.0004$ min^{-1}, $n = 80$), indicating less divalent cation influx.

recovery (efflux) could account for all of the changes in steady-state intracellular calcium following treatment with CSF_{tox}.

Pathways for calcium recovery

To provide an indication of the relative contribution of various calcium recovery processes to the long-term calcium destabilization seen after treatment with CSF_{tox}, we attempted to mimic the toxic process by treating cultures with inhibitors of each of the major recovery pathways. The effects of each inhibitor on neuronal calcium accumulation are summarized in Figure 4. Each curve is contrasted with the average effect of CSF_{tox} seen in parallel experiments (open circles). The potential contribution of organelle uptake of calcium by the endoplasmic reticulum and the mitochondria to acute and long-term calcium destabilization are illustrated in Figure 4A and B. Inhibition of ATP-dependent calcium transport into the endoplasmic reticulum by pretreatment with the inhibitor thapsigargin (1 μM) resulted in a small gradual increase in intracellular calcium that rose, significantly ($t = 9.06$, $df = 41$, $P < .001$), to a peak of 24% after about 3 min and remained relatively stable thereafter. Inhibition of mitochondrial respiration with carbonyl cyanide p-(trifluromethoxy)-

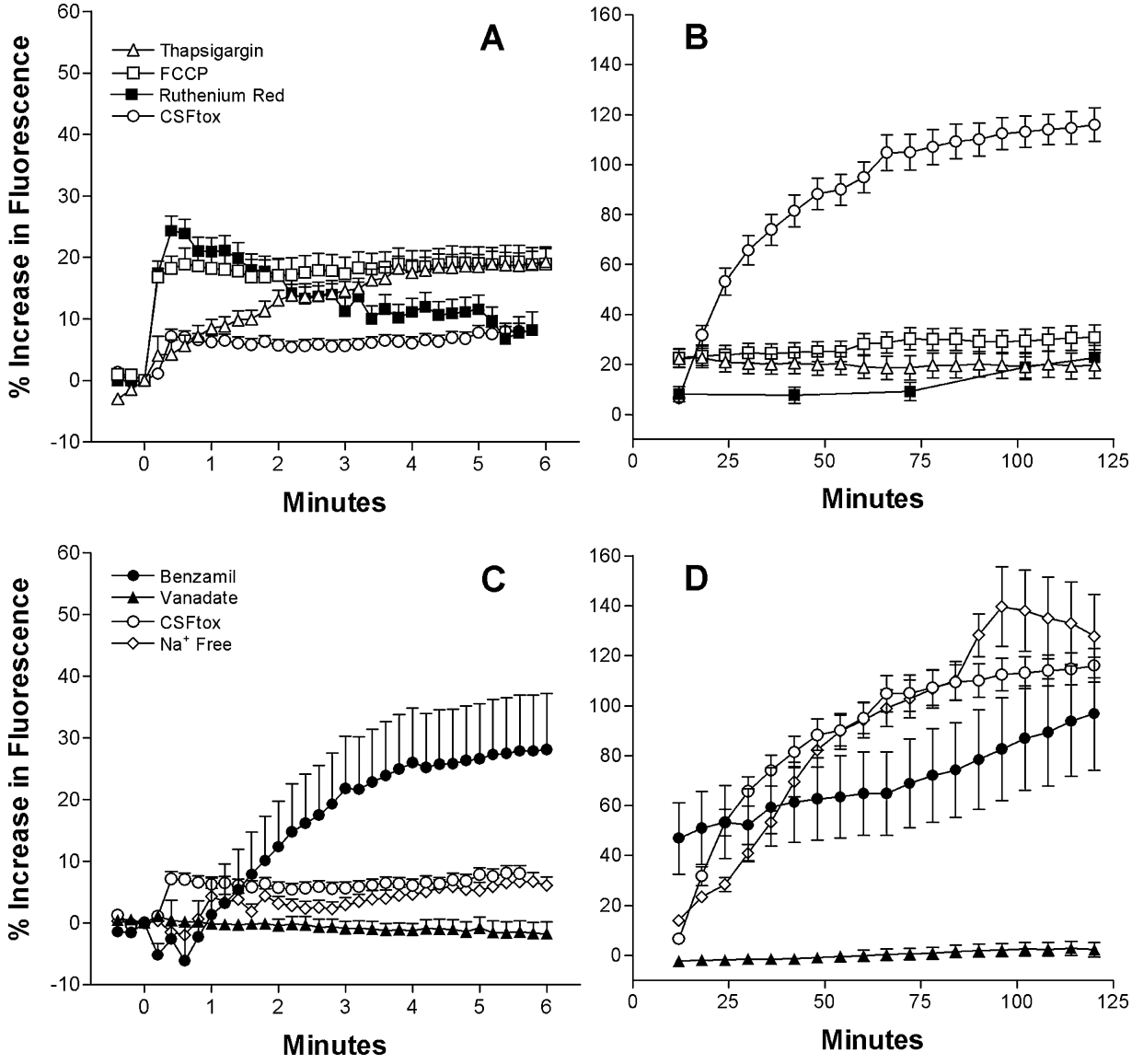

Figure 4 Changes in neuronal intracellular calcium in response to chronic blockade of the sarcoplasmic-endoplasmic reticulum ATPase, the mitochondrial uniporter, the plasma membrane calcium ATPase or the plasma membrane Na^+/Ca^{2+} exchanger. **A**, **B**, Inhibition of the sarcoplasmic endoplasmic reticulum ATPase by thapsigargin ($n = 42$) resulted in a gradual increase in intracellular calcium through the acute phase (**A**) that was mostly sustained throughout the long-term phase (**B**) (note the change in scale from acute to long-term). Inhibition of mitochondrial respiration with FCCP ($n = 62$) or the mitochondrial uniporter with ruthenium red ($n = 209$) both induced an acute increase in intracellular calcium that gradually recovered to baseline. None of these compounds achieved the long-term increase seen with CSF_{tox} (*open circles*, $n = 51$). **C**, **D**, Blockade of the plasma membrane calcium ATPase with orthovanadate (vanadate, $n = 41$) had a negligible average effect whereas inhibition of the Na^+/Ca^{2+} exchanger with benzamil ($n = 31$) or removal of extracellular Na^+ ($n = 78$) resulted in a small, gradual acute rise (**C**) followed by a large delayed increase in calcium that mimicked the increase seen with CSF_{tox}.(**D**).

phenylhydrazone (FCCP) resulted in a moderate, rapid increase in intracellular calcium that peaked at 20% ($t = 4.947$, $df = 61$, $P < .001$) and then decreased gradually to baseline. Ruthenium red, an antagonist of the ryanodyne receptor and mitochondrial calcium transport, also resulted in an acute peak of 24% ($t = 10.02$, $df = 208$, $P < .001$) followed by a decrease to near-baseline levels. A few cells showed late rises in calcium based on the criterion of a 70.7% increase established earlier for the response to CSF_{tox}: thapsigargin, 9.5%; FCCP, 8.6%; ruthenium red, 2.3%. This response frequency was similar to that seen in control cultures (4.8%). The potential contribution of plasma membrane calcium transport processes to calcium destabilization is illustrated in Figure 4C and D. Inhibition of the high-affinity plasma membrane calcium transporter with sodium orthovanadate (10 μM) had a negligible average effect on intracellular calcium accumulation, although some individual neurons exhibited a large delayed rise in calcium (4.2%). Inhibition of the plasma membrane Na^+/Ca^{2+} exchange with benzamil (500 μM)

induced a gradual and continuous rise in intracellular calcium that began after approximately 30 s and continued to rise through the acute phase of the experiment (Figure 4C; $t = 3.086$, $df = 30$, $P < .01$). The average maximum long-term rise in intracellular calcium of 97% ($t = 4.284$, $df = 30$, $P < .0001$ relative to basal) was similar to that seen following treatment with CSF_{tox}. The frequency of neurons responding to benzamil was 54.6%, slightly lower than the 69.8% seen with CSF_{tox}. To further evaluate the role of the Na^+/Ca^{2+} exchanger, the sodium gradient was reversed by the replacement of extracellular sodium with an equimolar concentration of *N*-methyl-*D*-glucamine (thereby inactivating the exchanger). In the relative absence of extracellular sodium, a very gradual acute rise ($t = 4.693$, $df = 31$, $P < .001$) was seen (Figure 4C) followed by a rapid delayed rise ($t = 8.769$, $df = 31$, $P < .001$; Figure 4D). The delayed increase was similar to that seen with benzamil and CSF_{tox}. The percentage of cells responding to the depletion of extracellular sodium with a delayed increase in calcium was slightly higher at 80.8% versus 69.8% for CSF_{tox} and 54.6% for benzamil. To verify that the calcium increases were due to the inability of the cell to recover from a calcium load, the kinetics of recovery were estimated following a pulse of 100 μM glutamate. The average rates of recovery in the presence of inhibitors of organelle calcium uptake or plasma membrane calcium efflux are summarized in Figure 5A and B, respectively. The average rate of recovery following glutamate-stimulated calcium uptake ($0.0649 \pm 0.0019\ s^{-1}$) was unaffected by ruthenium red ($-0.0594 \pm 0.0048\ s^{-1}$) but was accelerated 5.3-fold by thapsigargin ($-0.342 \pm 0.0216\ s^{-1}$; Figure 5A). Treatment with FCCP and orthovanadate slowed the initial rate of recovery by 1.5- to 1.8-fold relative to untreated cultures (Figure 5B). Benzamil (Figure 5B) caused the most dramatic slowing (24-fold) of the rate of intracellular calcium recovery ($-0.0027 \pm 0.0013\ s^{-1}$). Only a small reduction of calcium was seen over the first 6.5 min. At later time points, a significant rise in calcium was seen. Relative to controls, the extent of calcium recovery ranged from 88% to 122% after approximately 9.5 min for all drugs except benzamil. In the presence of benzamil, the maximal recovery was 13% and occurred at 4 min after the peak. This failure of cells to effectively clear intracellular calcium in the presence of benzamil suggests that the Na^+/Ca^{2+} exchanger performs most of this function under these conditions.

Discussion

How do HIV-associated toxins disable neurons?

A substantial body of work indicates that toxins released by macrophages and microglia contribute to the development of HIV encephalitis and HIV-associated dementia. Numerous studies indicate that the toxic activity involves glutamate receptor

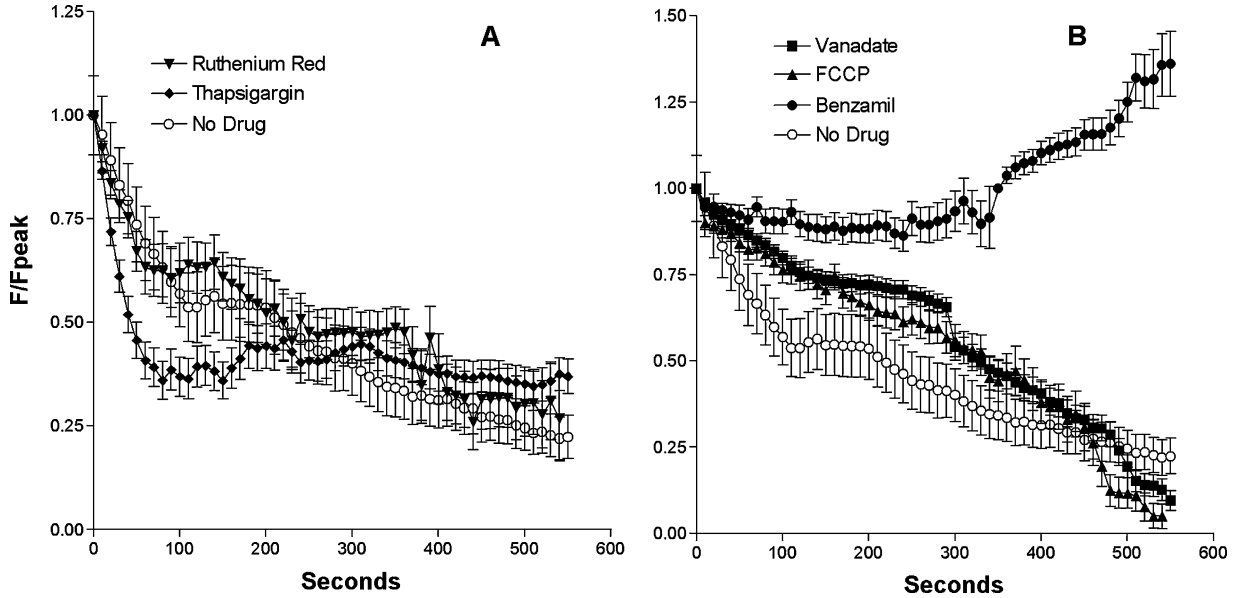

Figure 5 Intracellular calcium recovery in the presence of blockers of the sarcoplasmic endoplasmic reticulum ATPase, the mitochondrial uniporter, the plasma membrane calcium ATPase, or the plasma membrane Na^+/Ca^{2+} exchanger. Calcium recovery curves illustrate both rapid and slower recovery components. **A**, Thapsigargin ($n = 43$) evoked a transient acceleration of calcium clearance that lasted about 90 s whereas ruthenium red ($n = 11$) did not affect calcium recovery relative to neurons challenged in the absence of drug (No Drug, $n = 70$). Ruthenium red failed to show any difference in calcium recovery relative to the control curve (No Drug). **B**, Vanadate ($n = 67$) and FCCP ($n = 62$) both caused a slight, transient suppression of recovery that lasted approximately 6 min. Benzamil ($n = 22$) produced an almost complete suppression of calcium recovery acutely followed by an increase in intracellular calcium in the absence of any exogenous stimulation. Estimates of the initial recovery rates (0 to 5 min) indicated that the rate in benzamil was 24-fold lower than control neurons (No Drug).

activation (Haughey *et al*, 1999, 2001; Heyes *et al*, 1991; Holden *et al*, 1999; Lipton *et al*, 1991; Lipton, 1993; Nath and Geiger, 1998) and subsequent increases in intracellular calcium (Dreyer *et al*, 1990; Haughey *et al*, 1999; Holden *et al*, 1999; Nath *et al*, 1995; Navia *et al*, 1998). However, evidence implicating glutamate receptors has largely been indirect, showing that glutamate receptor antagonists suppress toxicity or that putative toxins indirectly facilitate the activation of glutamate receptors. For example, the actions of HIV-1 and FIV envelope proteins and the cytokine interleukin (IL)-6 appear to enhance the ability of glutamate to evoke increases in intracellular calcium while having no clear direct actions at glutamate receptors (Bernton *et al*, 1992; Bragg *et al*, 1999; Gruol *et al*, 1998; Lipton *et al*, 1991). Attempts to more clearly define the mechanisms that underlie cell injury present a complex picture in which numerous pharmacological agents acting through very different pathways have been shown to suppress toxicity. Antagonists that block increases in intracellular calcium accumulation through *N*-methyl-*D*-aspartate (NMDA) glutamate receptors or inositol triphosphate (IP_3)-regulated channels have been among the most potent compounds that protect neurons (Haughey *et al*, 1999; Holden *et al*, 1999; Lipton 1993), although substances that inhibit voltage-gated calcium channels (Dreyer *et al*, 1990; Holden *et al*, 1999), chemokine receptors (Zheng *et al*, 1999b), and Na^+/K^+ exchange (Holden *et al*, 1999) have also been shown to have protective efficacy. An obvious difficulty in the interpretation of these studies is that it has been hard to pin down a single pathway that might be primarily responsible for neurotoxicity and therefore might be an effective therapeutic target. A potential explanation for the apparent pharmacological diversity in the above studies is that each pathway may feed into a common intracellular end point that is disrupted by exposure to the virus and/or related toxins. The inability of the cell to clear intracellular calcium may represent this common end point and provide a unifying mechanism consistent with the pharmacological observations.

CSF_{tox} and intracellular calcium regulation

The ability of CSF_{tox} to suppress the clearance of intracellular calcium sets the stage for subsequent calcium accumulation in response to glutamate as well as numerous other substances that mobilize extracellular or intracellular calcium. The general nature of the dysfunction would explain the calcium dysregulation in astrocytes and microglia, as seen in Figures 1 and 2 and by others (Haughey *et al*, 1999; Holden *et al*, 1999), as well as the apparent dependence on synaptic transmission (Bragg *et al*, 2002b; Diop *et al*, 1994). Because the calcium overload represents an imbalance in the cytoplasmic calcium influx and efflux pathways, any antagonist that reduces the intracellular calcium burden would provide partial protection (e.g., see Bragg *et al*, 2002b) but would not eliminate the problem. In order for therapeutic strategies to be successful, the nature of the functional changes, including the identification of the putative microglial/macrophage toxins and their specific target(s) in the cell, that disable calcium regulation must be more clearly defined.

Potential targets of CSF_{tox}

There are four major pathways designed to remove calcium from the cytoplasm: the sarcoplasmic-endoplasmic reticulum Ca^{2+} ATPase (SERCA), the mitochondrial Ca^{2+} uniporter, the plasma membrane Ca^{2+} ATPase (PMCA), and the plasma membrane Na^+/Ca^{2+} exchanger (NCX). Although the pharmacological tools used for the assessment of calcium transport and exchange have limited specificities, each compound resulted in a unique pattern of calcium accumulation. Blockade of calcium uptake into the endoplasmic reticulum with thapsigargin resulted in a progressive, acute increase in intracellular calcium that was sustained at a fraction of the increase seen with CSF_{tox}. Inhibition of mitochondrial respiration with FCCP or blockade of calcium uptake by the uniporter resulted in an acute increase in intracellular calcium but only a negligible effect on the long-term regulation of calcium. These observations are consistent with the failure of thapsigargin to influence glutamate-elicited calcium transients (Kiedrowski and Costa, 1995) and the putative role of mitochondria in the regulation of acute calcium transients (Colegrove *et al*, 2000; Duchen, 2000; Vergun *et al*, 1999). Thus, although mitochondrial respiration and calcium transport into the endoplasmic reticulum are undoubtedly important for cell survival, deficits in these functions cannot easily explain the progressive increase in intracellular calcium in response to CSF_{tox} in the context of our experiments. Blockade of the ATP-dependent transport of calcium across the plasma membrane with orthovanadate also failed to provoke the same magnitude of calcium deregulation as CSF_{tox} and induced only a small transient reduction of the recovery rate. However, it should be noted that a few neurons (<5%) showed a pronounced deregulation of intracellular calcium in the presence of orthovanadate, suggesting that considerable variation may exist in the capacity for this mode of calcium transport in individual neurons. This observation is consistent with the identification of PMCA isoforms with different activities (Carafoli and Stauffer, 1994; Caride *et al*, 2001; Thayer *et al*, 2002) that participate in the rapid removal of small amounts of calcium.

The combined evidence from our studies indicated that only a dysfunction of the Na^+/Ca^{2+} exchanger was capable of generating the large delayed increase in intracellular calcium associated with CSF_{tox}. Benzamil, which preferentially inhibits the Na^+/Ca^{2+} exchanger, and inhibition of exchange activity by reversal of the transmembrane sodium gradient were the only treatments that mimicked the effects of the

CSF_{tox}. These observations are consistent with previous studies that suggest the Na^+/Ca^{2+} exchanger has a much larger calcium efflux capacity than the PMCA and accounts for regulation of cellular calcium homeostasis under a variety of physiological and pathological conditions (Castilho *et al*, 1999; Colegrove *et al*, 2000; Khodorov *et al*, 1993; Lu *et al*, 2002; Ranciat-McComb *et al*, 2000; Thayer *et al*, 2002).

Na^+/Ca^{2+} exchange and intracellular calcium overload

Three genetically distinct forms of the Na^+/Ca^{2+} exchanger designated NCX1, NCX2, and NCX3 have been identified in brain (Thurneysen *et al*, 2002), with NCX1 localized predominantly to neurons, NCX2 localized to glia (Thurneysen *et al*, 2002), and NCX3 limited to a subset of neurons. This distribution of NCX isoforms is consistent with effects of CSF_{tox} seen in neurons, astrocytes, and microglia and further suggests the possibility of different functional capabilities in different cells. Forward operation of the exchanger is activated following excitatory stimulation by glutamate (Khodorov *et al*, 1993; Yu and Choi, 1997) or other substances that increase intracellular calcium. Loss of exchanger activity due to oxidative damage (Huschenbett *et al*, 1998) and/or mitochondrial depolarization (Castilho *et al*, 1999) under conditions of excitotoxicity have been suggested to contribute to development of a poststimulation calcium plateau (Castilho *et al*, 1999; Colegrove *et al*, 2000; Vergun *et al*, 1999), delayed calcium deregulation, and death. A similar type of calcium plateau was seen with CSF_{tox} (Figure 3A) even after a brief subtoxic pulse of glutamate, indicating a shift toward an excitotoxic-like pattern. Thus, the physiological effects of Na^+/Ca^{2+} exchange inhibition may resemble excitotoxicity in many respects. However, because the downstream dysregulation of calcium is not strictly dependent on glutamate receptor stimulation, therapeutics directed to glutamate receptors or other individual upstream targets would be expected to have limited efficacy.

Changes in other calcium buffering processes could also contribute to the rise in intracellular calcium. Increased levels of calcium-binding proteins have been shown to decrease the rate of calcium rise (Chard *et al*, 1993) and have been shown to be neuroprotective in some (D'Orlando *et al*, 2002; McMahon *et al*, 1998) but not all (Isaacs *et al*, 2000; Mockel and Fisher, 1994) preparations. However, these proteins saturate quickly and are thought to provide acute local physiological modulation of action potentials (Jackson and Redman, 2003). In addition to the decrease in calcium rise, the kinetics of decay are slowed in the presence of excess calcium-binding proteins (Chard *et al*, 1993). These actions, thought to be protective, contrast with the effects of CSF_{tox} in which an extended, slow calcium decay is associated with deleterious effects. Thus, although a loss of calcium buffering could contribute to calcium accumulations, we do not believe such proteins are the major target of the actions of CSF_{tox}. It has also been suggested that reversal of the Na^+/Ca^{2+} exchanger following depolarization may contribute to intracellular calcium overload. The actions of CSF_{tox} on intracellular calcium accumulation is unlikely to be due to a reversal of the Na^+/Ca^{2+} exchanger because no acute effects are apparent that would be expected to promote exchange reversal and no evidence was found for increased calcium influx. This is consistent with the findings of Storozhevykh *et al* (1998) in which removal of external Na^+ greatly delayed calcium recovery in cerebellar granule cells after a glutamate challenge, with no indication of calcium influx due to reversed Na^+/Ca^{2+} exchange. Overall, evidence from various studies have indicated that the Na^+/Ca^{2+} exchanger plays an important role in maintaining intracellular calcium homeostasis under normal and pathological conditions. Toxin-induced loss of exchanger activity provides a compelling new theoretical framework compatible with the diverse body of literature on HIV-1–related toxins.

Materials and methods

Primary cultures of rat cortex

Pregnant female Long-Evans rats were lethally anesthetized in isoflurane and the uterus was removed and placed in ice cold HEPES-buffered Hank's balanced salt solution (HBSS). The fetuses (E17) were removed and the brain was harvested from the cranium of each fetus and rinsed three times in fresh sterile HBSS. The cerebral hemispheres containing the cortex and hippocampus were dissected in calcium-magnesium-free HBSS (CMF-HBSS), transferred to a 15-ml tube containing 5 ml CMF-HBSS + 1.25 U/ml dispase + 2 U/ml DNase I, and incubated for 20 min at 36°C. Tissue was then triturated by gentle passages through the tip of a 10-ml pipette. The cell pieces were allowed to settle for 2 min, and suspended cells were transferred to a 50-ml culture tube containing 25 ml of complete medium. The remaining tissue was resuspended in 3 to 5 ml CMF-HBSS and the trituration procedure repeated until most of the tissue was completely dispersed. The suspended cells were counted and seeded at a density 250,000 cells/cm^2 in each well of a 48-well plate for toxicity analysis and 40,000 cells/cm^2 on poly-D-lysine–treated coverslips for imaging. The resulting cultures were approximately 70% neurons on the first day after seeding and contained a mixed population of neurons, glia, and microglia at the time of testing. Cultures were fed by 50% medium exchange three times per week.

Preparation of CSF samples

CSF was collected from HIV+ patients prior to the introduction of highly active antiretroviral therapy (HAART). Immediately after collection, the CSF was centrifuged at 2500 rpm for 10 min and the cell-free

supernatant aliquoted and frozen at −80°C. Toxicity testing had previously been done on 30-kDa ultrafiltrates of the CSF, which removed virus and large proteins. These previous studies indicated that this ultrafiltrate retained all toxic activity (Meeker *et al*, 1999). Based on these earlier experiments, CSF was defined as toxic if cell death in the neural cultures was at least 2 standard deviations above the cell death seen in cultures treated with CSF from HIV-negative (HIV-) patients with no cognitive impairment (Meeker *et al*, 1999) or a preparation of artificial CSF. The artificial CSF was used as the vehicle for the CSF dilutions and proved to be the best standard for defining normal neuronal responses. Using this criterion, toxic CSF samples increased cell death in the cultures by 93% to 178% above the HIV− control CSF. Of these samples, 17% met the criterion for toxic activity. Toxic CSF from eight individuals was pooled to provide sufficient quantities of a consistent source for use in these experiments and is designated CSF_{tox}. The goal of these studies was to identify markers of toxic activity in the central nervous system (CNS) that develop during the early stages of pathogenesis. These studies (Meeker *et al*, 1999) and parallel animal studies (Bragg *et al*, 2002a) showed that the toxic activity appears early in the disease progression, well before the appearance of clinically significant neurological disease. The present experiments were intended to characterize the basic cellular processes that lead to neurotoxicity during these early stages of disease and were not designed to provide direct clinical correlations. Because of this, toxicity and not end-stage disease was used as a selection criterion for pooling the CSF. Consequently, the CSF samples with toxic activity could reflect all stages of HIV-associated disease. In Table 1, clinical information from the patients with toxic CSF is contrasted with all other HIV+ patients tested during the same time interval. Although these values provide a general indication of the underlying clinical picture associated with CSF_{tox}, it should be stressed that they currently have limited predictive value. On the average, CSF_{tox} induced over 10 times the cell death as the remaining CSF (112.9% ± 17.8% versus 9.8% ± 3.8% increase in cell death). Individuals from whom the CSF_{tox} was collected were slightly younger and had lower CD4 cell counts. Although dementia scores and neuropsychology scores were higher in the CSF_{tox} group, few had progressed to advanced stages of dementia (average score of 0.25 out of a maximum of 3). Both plasma HIV and the CSF HIV copy numbers were greater in the CSF_{tox}. There was also a tendency for the CSF:plasma ratio to be greater in the CSF_{tox}. Although on the surface this characterization suggests more rapid disease progression in the CSF_{tox} group, it is premature to draw such conclusions. Because the CSF was sampled during disease progression, we don't yet know the end point. We are continuing to follow these and other patients for a further and more extensive longitudinal characterization of the CSF.

Table 1 Clinical characteristics of patients from whom CSF_{tox} was collected relative to all HIV(+) individuals tested during the same period

	CSF_{tox}	*All HIV+*
Toxicity score	112.9 + 17.8	9.8 + 3.8 ($n = 76$)
Age (years)	36.5 + 1.6	41.7 + 3.3 ($n = 96$)
Demetia stage (0–3)	0.25 + 0.09	0.11 + 0.03 ($n = 93$)
Neuropsych score	93.69 + 23.10	53.83 + 5.02 ($n = 93$)
CD4 count	120.8 + 50.1	544.7 + 41.8 ($n = 94$)
Plasma HIV (copies/ml)	120959 + 91089	81224 + 29907 ($n = 40$)
CSF HIV (copies/ml)	3064 + 1558	800 + 389 ($n = 40$)
AIDS CDC score	1.75 + 0.16	0.91 + 0.11 ($n = 56$)

Note. CSF_{tox} was pooled from eight individuals. Toxicity scores reflect the average percent increase in cell death in neural cultures treated with the CSF relative to artifical CSF controls. The neuropsych score is a composite of neuropsychological tests, with the higher scores reflecting greater neuropsychological impairment.

Measurement of the effects of CSF_{tox} on neuronal calcium

Neuronal cultures were washed 2× in HEPES-buffered aCSF (concentrations in mM: NaCl 137, KCl 5.0, $CaCl_2$ 2.3, $MgCl_2$ 1.3, glucose 20, HEPES 10, adjusted to pH 7.4 with NaOH) and preloaded with the calcium indicator, Fluo-3 AM (2 to 4 μM, Molecular Probes, Eugene, OR) in serum-free medium. After 30 min, cultures were washed again, incubated in serum-free medium for an additional 10 minutes, then washed 2× in aCSF. The coverslips were removed from the culture dish and mounted in a specialized stage for imaging. Cells were maintained in 1.0 ml aCSF and imaged at a final magnification of 817×. Regions were selected to contain large cortical neurons as well as smaller neurons and microglia, if possible, for comparison. Time lapse digital images were captured automatically by the Metamorph System (Universal Imaging, Downingtown, PA). Three prestimulation measurements were taken to establish basal levels of fluorescence at the beginning of each experiment. These three readings ± SD were used to define the range of values considered to be basal calcium levels. The increase in fluorescence intensity within each cell was then measured relative to the baseline measurements to correct for cell to cell differences in dye loading and intrinsic fluorescence. Cells were stimulated by addition of 1 ml of a 1:10 dilution of CSF_{tox} (final dilution 1:20). A static bath was used to maintain exposure to the CSF_{tox}. Images were collected automatically to measure both acute and long-term changes in intracellular calcium. Control cultures were stimulated with vehicle in the same fashion as the CSF_{tox}.

Measurement of intracellular calcium recovery following a brief glutamate insult

Experiments designed to measure calcium recovery were done in a flow cell. Cultures preloaded with Fluo-3 were preexposed to CSF_{tox} (1:10 final dilution

to give maximal effect) for 10 min and then stimulated with a 6-s pulse of 100 μM glutamate in the presence of 10 μM glycine using pressure delivery of 100 μl from a glass micropipette. A continuous flow of aCSF (~0.5 ml/min) was used after the CSF_{tox} incubation to rapidly wash the glutamate from the culture. TTX (1 μM) was added to the aCSF to eliminate any influences from synaptic activity. To analyze the rates of recovery, the peak calcium level was determined (typically 6 to 12 s post stimulation) and designated $t = 0$. Neuronal fluorescence readings at all time points following the peak were divided by peak calcium (F/F_0). To estimate the rates of recovery, log (F/F_0) was plotted versus time and the rate constants (slope of the line) determined by regression analysis.

Pharmacology of calcium recovery

The following compounds were used to characterize the effect of various calcium recovery processes on intracellular calcium homeostasis: thapsigargin (1 μM), an inhibitor of the endoplasmic reticulum calcium pump; sodium orthovanadate (10 μM), an inhibitor of the plasma membrane calcium transporter; benzamil (200 μM), an inhibitor of the plasma membrane Na^+/Ca^{2+} exhanger; FCCP (1 μM), an inhibitor of mitochondrial oxidative phosphorylation and ruthenium red (1 μM), a putative blocker of ryanodine-sensitive calcium release and calcium uptake by the mitochondrial uniporter. These compounds were selected to provide the best possible block of the various pathways that contribute to intracellular calcium recovery, with the understanding that some are not highly specific. Concentrations were kept as low as possible to minimize overlapping actions at alternative sites. Measurement of direct effects of each drug was accomplished by perfusing the cells with drug after the third prestimulation image. In experiments designed to assess the effect of each antagonist on calcium recovery, the cells were pretreated for 15 min in 0.5 ml aCSF containing drug or vehicle plus 1 μM TTX. Three baseline levels were recorded and cells were challenged with a 6-s pulse of 100 μM glutamate. A continuous perfusion of aCSF (~0.5 ml/min) containing drug plus TTX was used to insure rapid washout of the glutamate and prevent contributions from synaptic activity. Digital images of the Fluo-3 fluorescence were captured at the indicated time points and fluorescence intensity measured in individual neurons over time.

References

Adamson DC, McArthur JC, Dawson TM, Dawson VL (1999). Rate and severity of HIV-associated dementia (HAD): correlations with Gp41 and iNOS. *Mol Med* **5:** 98–109.

Bernton EW, Bryant HU, Decoster MA, Orenstein JM, Ribas JL, Meltzer MS, Gendelman HE (1992). No direct neuronotoxicity by HIV-1 virions or culture fluids from HIV-1-infected T cells or monocytes. *Aids Res Hum Retroviruses* **8:** 495–503.

Bragg D, Hudson L, Liang Y, Tompkins M, Fernandes A, Meeker R (2002a). Choroid plexus macrophages proliferate and release toxic factors in response to feline immunodeficiency virus. *J NeuroVirol* **8:** 225–239.

Bragg DC, Boles JC, Meeker RB (2002b). Destabilization of neuronal calcium homeostasis by factors secreted from choroid plexus macrophage cultures in response to feline immunodeficiency virus. *Neurobiol Dis* **9:** 173–186.

Bragg DC, Meeker RB, Duff BA, English RV, Tompkins MB (1999). Neurotoxicity of FIV and FIV envelope protein in feline cortical cultures. *Brain Res* **816:** 431–437.

Brenneman DE, Westbrook GL, Fitzgerald SP, Ennist DL, Elkins KL, Ruff MR, Pert CB (1988). Neuronal cell killing by the envelope protein of HIV and its prevention by vasoactive intestinal peptide. *Nature* **335:** 639–642.

Carafoli E, Stauffer T (1994). The plasma membrane calcium pump: functional domains, regulation of the activity, and tissue specificity of isoform expression. *J Neurobiol* **25:** 312–324.

Caride AJ, Filoteo AG, Penheiter AR, Paszty K, Enyedi A, Penniston JT (2001). Delayed activation of the plasma membrane calcium pump by a sudden increase in Ca^{2+}: fast pumps reside in fast cells. *Cell Calcium* **30:** 49–57.

Castilho RF, Ward MW, Nicholls DG (1999). Oxidative stress, mitochondrial function, acute glutamate excitotoxicity in cultured cerebellar granule cells. *J Neurochem* **72:** 1394–1401.

Chard PS, Bleakman D, Christakos S, Fullmer CS, Miller RJ (1993). Calcium buffering properties of calbindin D28k and parvalbumin in rat sensory neurones. *J Physiol* **472**: 341–357.

Cheng J, Nath A, Knudsen B, Hochman S, Geiger JD, Ma M, Magnuson DS (1998). Neuronal excitatory properties of human immunodeficiency virus type 1 Tat protein. *Neuroscience* **82:** 97–106.

Colegrove SL, Albrecht MA, Friel DD (2000). Quantitative analysis of mitochondrial ca^{2+} uptake and release pathways in sympathetic neurons. Reconstruction of the recovery after depolarization-evoked [ca^{2+}]i elevations. *J Gen Physiol* **115:** 371–388.

Conant K, Garzino-Demo A, Nath A, McArthur JC, Halliday W, Power C, Gallo RC, Major EO (1998). Induction of monocyte chemoattractant protein-1 in HIV-1 Tat-stimulated astrocytes and elevation in AIDS dementia. *Proc Natl Acad Sci U S A* **95:** 3117–3121.

Diop AG, Lesort M, Esclaire F, Sindou P, Couratier P, Hugon J (1994). Tetrodotoxin blocks HIV coat protein (gp120) toxicity in primary neuronal cultures. *Neurosci Lett* **165:** 187–190.

D'Orlando C, Celio MR, Schwaller B (2002). Calretinin and calbindin D-28k, but not parvalbumin, protect against glutamate-induced delayed excitotoxicity in transfected N18-RE 105 neuroblastoma-retina hybrid cells. *Brain Res* **945:** 181–190.

Dreyer E, Kaiser P, Offerman J, Lipton S (1990). HIV-1 coat protein neurotoxicity prevented by calcium channel antagonists. *Science* **248:** 364–367.

Duchen MR (2000). Mitochondria and calcium: from cell signalling to cell death. *J Physiol* **529(Pt 1):** 57–68.

Gelbard HA, Nottet HS, Swindells S, Jett M, Dzenko KA, Genis P, White R, Wang L, Choi Y-B, Zhang D, Lipton SA, Tourtellotte WW, Epstein LG, Gendelman HE (1994). Platelet-activating factor: a candidate human immunodeficiency virus type 1-induced neurotoxin. *J Virol* **68:** 4628–4635.

Genis P, Jett M, Bernton EW (1992). Cytokines and arachidonic metabolites produced during human immunodeficiency virus (HIV)-infected macrophage-astroglia interactions: implications for the neuropathogenesis of HIV disease. *Exp Med* **176:** 1703–1718.

Giulian D, Vaca K, Noonan CA (1990). Secretion of neurotoxins by mononuclear phagocytes infected with HIV-1. *Science* **250:** 1593–1596.

Giulian D, Yu J, Li X, Tom D, Li J, Wendt E, Lin S-N, Schwarcz R, Noonan C (1996). Study of receptor-mediated neurotoxins released by HIV-1-infected mononuclear phagocytes found in human brain. *J Neurosci* **16:** 3139–3153.

Graziosi C, Gantt KR, Vaccarezza M, Demarest JF, Daucher M, Saag MS, Shaw GM, Quinn TC, Cohen OJ, Welbon CC, Pantaleo G, Fauci AS (1996). Kinetics of cytokine expression during primary human immunodeficiency virus type 1 infection. *Proc Natl Acad Sci U S A* **93:** 4386–4391.

Grimaldi LM, Martino GV, Franciotta DM, Brustia R, Castagna A, Pristera R, Lazzarin A (1991). Elevated alpha-tumor necrosis factor levels in spinal fluid from HIV-1 infected patients with central nervous system involvement. *Ann Neurol* **29:** 21–25.

Gruol DL, Yu N, Parsons KL, Billaud JN, Elder JH, Phillips TR (1998). Neurotoxic effects of feline immunodeficiency virus, FIV-PPR. *J NeuroVirol* **4:** 415–425.

Haughey NJ, Holden CP, Nath A, Geiger JD (1999). Involvement of inositol 1,4,5-trisphosphate-regulated stores of intracellular calcium in calcium dysregulation and neuron cell death caused by HIV-1 protein tat. *J Neurochem* **73:** 1363–1374.

Haughey NJ, Nath A, Mattson MP, Slevin JT, Geiger JD (2001). HIV-1 Tat through phosphorylation of NMDA receptors potentiates glutamate excitotoxicity. *J Neurochem* **78:** 457–467.

Hesselgesser J, Taub D, Baskar P, Greenberg M, Hoxie J, Kolson DL, Horuk R (1998). Neuronal apoptosis induced by HIV-1 gp120 and the chemokine SDF-1 alpha is mediated by the chemokine receptor CXCR4. *Curr Biol* **8:** 595–598.

Heyes MP, Brew BJ, Martin A, Price RW, Salazar AM, Sidtis JJ, Yergey JA, Mouradian MM, Sadler AE, Keilp J, Rubinow D, Markey SP (1991). Quinolinic acid in cerebrospinal fluid and serum in HIV-1 infection: relationship to clinical and neurological status. *Ann Neurol* **29:** 202–209.

Holden CP, Haughey NJ, Nath A, Geiger JD (1999). Role of Na^+/H^+ exchangers, excitatory amino acid receptors and voltage-operated ca^{2+} channels in human immunodeficiency virus type 1 gp120-mediated increases in intracellular ca^{2+} in human neurons and astrocytes. *Neuroscience* **91:** 1369–1378.

Huschenbett J, Zaidi A, Michaelis ML (1998). Sensitivity of the synaptic membrane Na^+/ca^{2+} exchanger and the expressed NCX1 isoform to reactive oxygen species. *Biochim Biophys Acta* **1374:** 34–46.

Isaacs KR, Wolpoe ME, Jacobowitz DM (2000). Vulnerability to calcium-induced neurotoxicity in cultured neurons expressing calretinin. *Exp Neurol* **163**: 311–323.

Jackson MB, Redman SJ (2003). Calcium dynamics, buffering, and buffer saturation in the boutons of dentate granule-cell axons in the hilus. *J Neurosci* **23**: 1612–1621.

Kaul M, Garden GA, Lipton SA (2001). Pathways to neuronal injury and apoptosis in HIV-associated dementia. *Nature* **410:** 988–994.

Kelder W, McArthur JC, Nance-Sproson T, McClernon D, Griffin DE (1998). Beta-chemokines MCP-1 and RANTES are selectively increased in cerebrospinal fluid of patients with human immunodeficiency virus-associated dementia. *Ann Neurol* **44:** 831–835.

Khodorov B, Pinelis V, Golovina V, Fajuk D, Andreeva N, Uvarova T, Khaspekov L, Victorov I (1993). On the origin of a sustained increase in cytosolic ca^{2+} concentration after a toxic glutamate treatment of the nerve cell culture. *FEBS Lett* **324:** 271–273.

Kiedrowski L, Costa E (1995). Glutamate-induced destabilization of intracellular calcium concentration homeostasis in cultured cerebellar granule cells: role of mitochondria in calcium buffering. *Mol Pharmacol* **47:** 140–147.

Lipton S (1992). Requirement of macrophages in neuronal injury induced by HIV envelope protein gp120. *NeuroReport* **3:** 913–915.

Lipton S (1993). Prospects for clinically tolerated NMDA antagonists: open-channel blockers and alternative redox states of nitric oxide. *Trends Neurosci* **16:** 527–532.

Lipton S, Sucher N, Kaiser P, Dreyer E (1991). Synergistic effects of HIV coat protein and NMDA receptor-mediated neurotoxicity. *Neuron* **7:** 111–118.

Lu J, Tong XY, Wang XL (2002). Altered gene expression of Na^+/ca^{2+} exchanger isoforms NCX1, NCX2 and NCX3 in chronic ischemic rat brain. *Neurosci Lett* **332:** 21–24.

Magnuson D, Knudsen B, Geiger J, Brownstone R, Nath A (1995). Human immunodeficiecy virus type 1 Tat activates non-*N*-methyl-D-aspartate excitatory amino acid receptors and causes neurotoxicity. *Ann Neurol* **37:** 373–380.

McMahon A, Wong BS, Iacopino AM, Ng MC, Chi S, German DC (1998). Calbindin-D28k buffers intracellular calcium and promotes resistance to degeneration in PC12 cells. *Brain Res Mol Brain Res* **54**: 56–63.

Meeker RB, Robertson K, Barry T, Hall C (1999). Neurotoxicity of CSF from HIV-infected humans. *J NeuroVirol* **5:** 507–518.

Mockel V, Fischer G (1994). Vulnerability to excitotoxic stimuli of cultured rat hippocampal neurons containing the calcium-binding proteins calretinin and calbindin D28K. *Brain Res* **648:** 109–120.

Nath A, Geiger J (1998). Neurobiological aspects of human immunodeficiency virus infection: neurotoxic mechanisms. *Prog Neurobiol* **54:** 19–33.

Nath A, Pauda RA, Geiger JD (1995). HIV-1 coat protein gp120-induced increases in levels of intrasynaptosomal calcium. *Brain Res* **678:** 200–206.

Navia BA, Dafni U, Simpson D, Tucker T, Singer E, McArthur JC, Yiannoutsos C, Zaborski L, Lipton SA (1998). A phase I/II trial of nimodipine for HIV-related neurologic complications. *Neurology* **51:** 221–228.

New DR, Ma M, Epstein LG, Nath A, Gelbard HA (1997). Human immunodeficiency virus type 1 Tat protein induces death by apoptosis in primary human neuron cultures. *NeuroVirol* **3:** 168–173.

Perrella O, Carrieri PB, Guarnaccia D, Soscia M (1992). Cerebrospinal fluid cytokines in AIDS dementia complex. *J Neurol* **239:** 387–388.

Pulliam L, Clarke JA, McGuire D, McGrath MS (1994). Investigation of HIV-infected macrophage neurotoxin production from patients with AIDS dementia. *Adv Neuroimmunol* **4:** 195–198.

Ranciat-McComb NS, Bland KS, Huschenbett J, Ramonda L, Bechtel M, Zaidi A, Michaelis ML (2000). Antisense oligonucleotide suppression of Na(+)/Ca(2+) exchanger activity in primary neurons from rat brain. *Neurosci Lett* **294:** 13–16.

Storozhevykh T, Grigortsevich N, Sorokina E, Vinskaya N, Vergun O, Pinelis V, Khodorov B (1998). Role of Na^{2+}/ca^{2+} exchange in regulation of neuronal ca^{2+} homeostasis requires re-evaluation. *FEBS Lett* **431:** 215–218.

Thayer SA, Usachev YM, Pottorf WJ (2002). Modulating ca^{2+} clearance from neurons. *Front Biosci* **7:** d1255–d1279.

Thurneysen T, Nicoll DA, Philipson KD, Porzig H (2002). Sodium/calcium exchanger subtypes NCX1, NCX2 and NCX3 show cell-specific expression in rat hippocampus cultures. *Brain Res Mol Brain Res* **107:** 145–156.

Vergun O, Keelan J, Khodorov BI, Duchen MR (1999). Glutamate-induced mitochondrial depolarisation and perturbation of calcium homeostasis in cultured rat hippocampal neurones. *J Physiol* **519(Pt 2):** 451–466.

Wesselingh SL, Takahashi K, Glass JD, McArthur JC, Griffin JW, Griffin DE (1997). Cellular localization of tumor necrosis factor mRNA in neurological tissue from HIV-infected patients by combined reverse transcriptase/polymerase chain reaction in situ hybridization and immunohistochemistry. *J Neuroimmunol* **74:** 1–8.

Xiong H, Zeng YC, Lewis T, Zheng J, Persidsky Y, Gendelman HE (2000). HIV-1 infected mononuclear phagocyte secretory products affect neuronal physiology leading to cellular demise: relevance for HIV-1-associated dementia. *J NeuroVirol* **6(Suppl 1):** S14–S23.

Yeung MC, Pulliam L, Lau AS (1995). The HIV envelope protein gp120 is toxic to human brain-cell cultures through the induction of interleukin-6 and tumor necrosis factor-alpha. *AIDS* **9:** 137–143.

Yu SP, Choi DW (1997). Na^{+}-ca^{2+} exchange currents in cortical neurons: concomitant forward and reverse operation and effect of glutamate. *Eur J Neurosci* **9:** 1273–1281.

Zheng J, Ghorpade A, Niemann D, Cotter RL, Thylin MR, Epstein L, Swartz JM, Shepard RB, Liu X, Nukuna A, Gendelman HE (1999a). Lymphotropic virions affect chemokine receptor-mediated neural signaling and apoptosis: implications for human immunodeficiency virus type 1-associated dementia. *J Virol* **73:** 8256–8267.

Zheng J, Thylin MR, Ghorpade A, Xiong H, Persidsky Y, Cotter R, Niemann D, Che M, Zeng YC, Gelbard HA, Shepard RB, Swartz JM, Gendelman HE (1999b). Intracellular CXCR4 signaling, neuronal apoptosis and neuropathogenic mechanisms of HIV-1-associated dementia. *J Neuroimmunol* **98:** 185–200.